



**HAL**  
open science

## **Dislocation mobility in gum metal $\beta$ -titanium alloy studied via in situ transmission electron microscopy**

Philippe Castany, Magali Besse, Thierry Gloriant

### ► **To cite this version:**

Philippe Castany, Magali Besse, Thierry Gloriant. Dislocation mobility in gum metal  $\beta$ -titanium alloy studied via in situ transmission electron microscopy. *Physical Review B: Condensed Matter and Materials Physics* (1998-2015), 2011, 84 (2), pp.201-1 - 201-4. <10.1103/PhysRevB.84.020201>. <hal-00864948>

**HAL Id: hal-00864948**

**<https://hal.science/hal-00864948v1>**

Submitted on 24 Sep 2013

**HAL** is a multi-disciplinary open access archive for the deposit and dissemination of scientific research documents, whether they are published or not. The documents may come from teaching and research institutions in France or abroad, or from public or private research centers.

L'archive ouverte pluridisciplinaire **HAL**, est destinée au dépôt et à la diffusion de documents scientifiques de niveau recherche, publiés ou non, émanant des établissements d'enseignement et de recherche français ou étrangers, des laboratoires publics ou privés.



HAL Authorization

# **Dislocation mobility in gum metal $\beta$ -titanium alloy studied via in situ transmission electron microscopy**

P. Castany\*, M. Besse, T. Gloriant

INSA de Rennes, UMR CNRS 6226 Sciences Chimiques de Rennes/Chimie-Métallurgie, 20 avenue des Buttes de Coësmes, CS70839, 35708 Rennes Cedex 7, France

*In situ* tensile tests in a transmission electron microscope were carried out on a “Gum Metal”  $\beta$  titanium alloy. Conventional dislocation slip was observed to be the only mechanism occurring during the plastic deformation. The low mobility of screw dislocations was shown to be due to their core structure configuration. Nanometer-sized obstacles were also present but have a weaker effect of the dislocation mobility. The density of these obstacles and the variation in energy due to the core structure of screw dislocations were measured and compared to theoretical data of literature.

## **I. INTRODUCTION**

Recently, a new group of metastable  $\beta$  titanium alloys, called Gum Metals, has been developed.<sup>1</sup> These multifunctional alloys are shown to possess “super”-properties such as very high strength, low Young’s modulus, superelasticity and superplasticity at room temperature. Some of these properties are obtained after cold working and are supposed to be due to nonconventional dislocation-free deformation mechanisms: “nanodisturbances” (distorted nano-areas)<sup>1,2</sup> and “giant faults” (pure shear bands).<sup>1,3</sup> Occurrence of these unique plastic deformation mechanisms is assumed to be due to the very low value of ideal shear stress that is comparable to the applied stress.<sup>1,4</sup> Consequently, these alloys would reach their ideal stress before the critical shear stress of conventional dislocation slip is reached that allows the crystal to be sheared without dislocation activity (by giant faults and

nanodisturbances). These alloys are thus supposed to deform plastically without conventional dislocation slip. This peculiar property is possible if the glide of conventional dislocations is inhibited when a mechanical stress is applied. Two hypotheses have been proposed to explain this point. First, it was assumed that dislocations are pinned by a large density of nano-sized obstacles<sup>4</sup> such as ZrO atom clusters,<sup>1</sup> solute atoms<sup>2</sup> or nano-scale  $\omega$  phase.<sup>5,6</sup> Secondly, it was also proposed that screw dislocations have a non-planar split core structure that strongly reduced their mobility.<sup>7</sup> The remarkable mechanical properties after cold working are then thought to be due to the specific microstructure obtained from the aggregation of giant faults during severe deformation.<sup>1,3</sup> Giant faults are observed in annealed specimens<sup>1,3</sup> as well as in cold worked specimens.<sup>2,3</sup> However, further studies have shown that dislocations are present in these alloys and possibly contribute to plastic deformation.<sup>8-11</sup> Twinning and stress induced martensitic transformation are also observed.<sup>10,12,13</sup> Recent calculations also demonstrated that the overlapping of cores of near screw dislocations lead to an atomic arrangement similar to the nanodisturbances observed in cold worked Gum Metals.<sup>14</sup>

Some controversy regarding the deformation mechanisms operating in Gum Metals still remains and the role of dislocations slip in the plastic deformation has not been evidenced. In the present study, *in situ* tensile tests in a transmission electron microscope (TEM) are thus carried out to investigate the mechanisms of deformation in a Gum Metal. The parameters that control the mobility of dislocations are also investigated.

## II. EXPERIMENTAL PROCEDURE

A Gum Metal with the composition Ti-23Nb-0.7Ta-2Zr-1.2O (at. %) was elaborated by cold crucible levitation melting (CCLM) of pure raw materials. Ingots were next homogenized at 1223 K during 16 hours, 90% cold rolled, recrystallized at 1143 K during 0.5 hour and water quenched. The microstructure consists of equiaxed grains of  $\beta$  phase (bcc) with an average size of 40  $\mu\text{m}$ . This alloy exhibits the typical mechanical properties of Gum Metals:<sup>1,15</sup> a yield strength of 830 MPa, a Young's Modulus of 60 GPa and an elastic strain of 1.5%.<sup>16</sup>

*In situ* tensile tests were performed at room temperature in a JEOL 2010 TEM operating at 200 kV using a Gatan straining holder. *In situ* observations were recorded with a SIS CCD camera for video rate recording. Dimensions of micro tensile specimens are 9mm  $\times$  2.3mm  $\times$  80 $\mu\text{m}$ . They were thinned down in the centre of the reduced section using a twin-jet

electropolishing system with a solution of 6% perchloric acid, 59% methanol and 35% 2-butoxyethanol (vol.%).

### III. RESULTS AND DISCUSSION

During *in situ* tensile tests, conventional dislocation slip is the only deformation mechanism observed. No giant faults, twinning or stress induced martensitic transformation are observed. Fig. 1 is a picture of mobile dislocations taken from a video recorded during an *in situ* experiment. There was no dislocation before straining. Dislocations are first emitted from grain boundaries and propagate next within grains. They multiply by the well-known open loop mechanism which is due to double cross-slip<sup>17,18</sup> and results in the presence of numerous expanding dislocation loops (arrowed in Fig. 1). All mobile dislocations have  $a/2\langle 111 \rangle$  Burgers vectors, which were determined by regular indexation using the invisibility criterion. Slip planes are determined by the analysis of slip traces left by dislocations on the surface of the thin foil (labelled “trace” on Fig. 1 and 2a). As in most of bcc metals, slip planes are observed to be  $\{110\}$  or  $\{112\}$  planes. Several slip systems are frequently observed to operate in the same grain. Some of slip traces are wavy as a result of multiple and intensive cross-slip that is in agreement with the occurrence of the open loop multiplication mechanism. The velocity of screw segments is observed to be much lower than the velocity of non-screw segments. Consequently, the latter quickly move out of the thin foil and the screw dislocation density increases. The deformation rate is then mainly controlled by the low mobility of screw dislocations.

#### A. Core structure of screw dislocations

To determine the parameters responsible of the low mobility of screw dislocations, a precise analysis of their motion is necessary. Fig. 2 shows an example of a frame by frame analysis of this motion. Screw segments appear to have a jerky motion consisting of successive jumps of parts of the screw dislocation (see supplementary movie 1<sup>19</sup> that corresponds to the Fig. 2). Between two consecutive jumps, the dislocation remains perfectly immobile. Each frame of Fig. 2 corresponds to a jump of a part of a screw dislocation; the time of a jump is shorter than a video frame (0.04s). This jerky motion of screw dislocations is also observed in various

bcc metals<sup>17,20,21</sup> and in  $\alpha$  titanium phase.<sup>18,22</sup> This kind of motion is known to be due to a transition from a stable and sessile three-dimensionally spread core structure (that corresponds to the immobile state) to a metastable and glissile state (that corresponds to rapid jumps). In pure bcc metals, this jerky motion is observed at low temperature and the whole screw segment jumps.<sup>17,20,21</sup> In the present Gum Metal (bcc titanium phase), the jerky motion is observed at room temperature. That means this mechanism occurs in a larger temperature range than in pure bcc metals: this is probably due to the presence of alloying elements that makes the sessile-glissile transition more difficult than in pure metals.

Moreover, in the present study, it is observed that screw dislocations jump by successive parts instead of the jump of the whole dislocation as commonly observed in pure bcc metals. When a part of the dislocation moves, pinning points impeding its motion are clearly visible (Fig. 2). These pinning points are extrinsic and their role and density will be discussed in the following paragraph. However, their presence has a relatively weak effect on the mobility of screw dislocations in comparison with the effect of their core structure.

The energy gap between the two core configurations is then the detrimental parameter responsible of the lower mobility of screw dislocations. Existence of such an energy gap causes the preferential orientation of dislocations along their screw direction. The change of the dislocation direction between the screw part and the non-screw one is then abrupt in comparison with the pseudo-elliptic shape of a conventional dislocation calculated from anisotropic elasticity. The angle of this change in direction can be easily measured from *in situ* TEM tensile tests on dislocations under stress and just before they unlock their screw position to another one (Fig. 2d for example). Its value can next be related to the energy gap (see Ref. <sup>23</sup> for more details on this method). This escape angle from the screw orientation is then measured to be  $\varphi = 24^\circ \pm 2^\circ$ . The relative variation in energy  $\Delta E_s/E_s$ , where  $E_s$  is the anisotropic elastic energy of a screw dislocation, is then calculated from the value of  $\varphi$ . The experimental elastic constants of a same composition alloy are used for calculations.<sup>24</sup> The escape angle of  $\varphi = 24^\circ$  corresponds then to an energy variation  $\Delta E_s/E_s = 18\% \pm 3\%$ . Taking the value  $E_s = 3.23 \times 10^{-10} \text{ J.m}^{-1} = 2.02 \text{ eV.nm}^{-1}$  of the elastic energy of a screw dislocation calculated from the DISDI software,<sup>25,26</sup> the value of the variation in energy is calculated to be  $\Delta E_s = 0.36 \pm 0.06 \text{ eV.nm}^{-1}$ . This variation in energy corresponds to the gap, due to the three-dimensionally spread core structure, that dislocations have to overcome to glide.

Bobylev et al. suggested a non planar spreading of the core of screw dislocations in Gum Metal and calculated the difference between energies of respectively a non-split and a split

core configuration.<sup>7</sup> This value was found to be about  $0.2 \text{ eV.nm}^{-1}$  (depending on the core configuration chosen) and can be attributed to the gain in energy obtained by dislocations when their core has a spread and stable configuration. This gain corresponds to the variation in energy  $\Delta E_s$  that we measured experimentally in the present study. Both values are quite similar confirming the hypothesis of a spread core structure of screw dislocations in Gum Metals. However, Bobylev et al. considered this spreading sufficient to inhibit any motion of dislocations<sup>7</sup> while we demonstrate here that this gap in energy is overcome when a stress is applied. Nevertheless, screw dislocations can only maintain a gliding configuration for very short time (less than 0.04 s) leading to a jerky motion during which dislocations core is mainly in its spread configuration. As the energy difference increases when dislocation core splits into an increasing number of partials<sup>7</sup> and as we measure a value  $\Delta E_s$  larger than the value for a core split into 12 partials (respectively  $0.36$  and  $0.2 \text{ eV.nm}^{-1}$ ), one can assume that the core is split in more partials, i.e. it tends to a continuous spreading. Continuous core spreading has been considered recently from atomistic simulations in Gum Metal but energy values are unfortunately not available to be compared with our experimental data.<sup>14</sup> Nevertheless, present results suggest that a continuous spread core configuration seems energetically more accurate than a core configuration split into partials.

### B. Nanometer-sized pinning obstacles

As pointed out from the motion of screw dislocations, some pinning points are observable on dislocations. However, these obstacles have not an important effect on the screw dislocation mobility in comparison with their core structure. To analyse the role of these pinning points, the motion of non-screw segments have to be considered. We showed previously that non-screw dislocations are not easily observable during straining experiments due to their high mobility. But when the straining is stopped (still under stress) stress relaxation occurred and the velocity of dislocations decreases enough to make the motion of non-screw segments observable. An example of non-screw  $a/2\langle 111 \rangle$  dislocations gliding in  $\{110\}$  plane is shown in Fig. 3 (corresponding to supplementary movie 2<sup>27</sup>). Their motion is clearly impeded by the presence of a dense distribution of pinning obstacles arrowed in Fig. 3. The density of such obstacles in  $\{110\}$  slip planes can be measured by counting the number of pinning points swept by dislocations during their motion. The average surface density  $n_s$  in  $\{110\}$  planes is

870 pinning points per  $\mu\text{m}^2$ . Assuming an homogeneous distribution, the average spacing between pinning points  $d_S$  can be estimated from the following relation:<sup>28</sup>

$$d_S = \frac{1}{2\sqrt{n_S}}$$

The mean spacing  $d_S$  in  $\{110\}$  planes is thus measured to be 17 nm. The critical distance  $l_c$  between obstacles has been calculated for Gum Metals,<sup>4</sup> i.e. if the distance between obstacles is less than  $l_c$ , dislocations are pinned without the possibility to be unpinned before the material reached its ideal shear stress and then deformed plastically without dislocation slip. Taking the value  $e/a = 4.25$  (valence electron-atom ratio) corresponding to Gum Metals, the critical distance  $l_c$  in  $\{110\}$  planes is obtained from:<sup>4</sup>  $l_c = 2$  nm for screw  $a/2\langle 111 \rangle$  dislocations and  $l_c = 6$  nm for edge ones. The spacing  $d_S$  between obstacles is then measured to be three times larger than  $l_c$  for edge dislocations and dislocations are clearly able to overcome these obstacles before the ideal shear stress is reached. Nevertheless, the values of  $d_S$  and  $l_c$  are very close and one can assume that ideal shear stress can be reached in cold worked materials. Indeed, forest dislocations formed during cold working are additional obstacles for mobile dislocations that increase the obstacle density and could allow the material to deform via pure shear (giant faults) without dislocation slip as previously observed.<sup>1</sup>

In the literature, pinning obstacles to dislocation motion are attributed to ZrO atom clusters<sup>1</sup> or nanometer-sized  $\omega$  precipitates.<sup>5,6</sup> In the present study, no characteristic extra diffuse spots of  $\omega$  phase are observed in diffraction patterns and we assume that pinning points are atom clusters. However, Yano et al. reported that  $\omega$  phase is induced during cold working in Gum Metals.<sup>5</sup> Atom clusters are thus most probably precursors to  $\omega$  phase. This assumption is supported by the average volume density of pinning points that is quite similar to the volume density of nanometer-sized  $\omega$  phase in cold worked Gum Metal ( $1.3 \times 10^{-3} \text{ nm}^{-3}$ ).<sup>6</sup> Indeed, the volume density  $n_V$  of obstacles swept by mobile dislocations during *in situ* TEM experiments can be extrapolated from their surface density  $n_S$  in  $\{110\}$  planes by dividing its value by the spacing between  $\{110\}$  planes. Thus, the value is  $n_V = 3.7 \times 10^{-3} \text{ nm}^{-3}$ . It is also worth noting that the corresponding mean spacing of obstacles in the volume  $d_V$  is calculated to be 4 nm. But, to predict the pinning of dislocations, the mean spacing of obstacles in the slip plane of dislocations  $d_S$  (17 nm) have to be used<sup>4</sup> instead of the volume mean spacing  $d_V$  (4 nm).

## IV. CONCLUSION

As a summary, we demonstrated that Gum Metal  $\beta$  titanium alloys deform plastically via conventional dislocation slip. Screw dislocations are shown to have a lower mobility than non-screw segments. This low mobility is due to their spread core structure that has to recombine to glide. The mobility of dislocations is quite similar to that in other bcc metals. A large density of nanometer-sized obstacles impeded the motion of non-screw dislocations at low stress, but their density is too low to have a critical effect on the mobility of dislocations at higher stress. The ideal strength is thus not reached before dislocation slip is activated and dislocations carried the plastic deformation in the annealed state.

## ACKNOWLEDGMENTS

The authors acknowledge financial support from the French CNRS and CEA METSA network for *in situ* TEM experiments.

\* philippe.castany@insa-rennes.fr

<sup>1</sup>T. Saito, *et al.*, *Science* **300**, 464 (2003).

<sup>2</sup>M. Y. Gutkin, T. Ishizaki, S. Kuramoto, and I. A. Ovid'ko, *Acta Mater.* **54**, 2489 (2006).

<sup>3</sup>M. Y. Gutkin, T. Ishizaki, S. Kuramoto, I. A. Ovid'ko, and N. V. Skiba, *Int. J. Plast.* **24**, 1333 (2008).

<sup>4</sup>T. Li, J. W. Morris, N. Nagasako, S. Kuramoto, and D. C. Chrzan, *Phys. Rev. Lett.* **98**, 105503 (2007).

<sup>5</sup>T. Yano, Y. Murakami, D. Shindo, and S. Kuramoto, *Acta Mater.* **57**, 628 (2009).

<sup>6</sup>T. Yano, Y. Murakami, D. Shindo, Y. Hayasaka, and S. Kuramoto, *Scripta Mater.* **63**, 536 (2010).

<sup>7</sup>S. V. Bobylev, T. Ishizaki, S. Kuramoto, and I. A. Ovid'ko, *Phys. Rev. B* **77**, 094115 (2008).

<sup>8</sup>H. Xing, J. Sun, Q. Yao, W. Y. Guo, and R. Chen, *Appl. Phys. Lett.* **92**, 151905 (2008).

<sup>9</sup>W. Y. Guo, H. Xing, J. Sun, X. L. Li, J. S. Wu, and R. Chen, *Metall. Mater. Trans. A* **39**, 672 (2008).

<sup>10</sup>Y. Yang, S. Q. Wu, G. P. Li, Y. L. Li, Y. F. Lu, K. Yang, and P. Ge, *Acta Mater.* **58**, 2778 (2010).

<sup>11</sup>E. Withey, M. Jin, A. Minor, S. Kuramoto, D. C. Chrzan, and J. W. Morris Jr, *Mater. Sci. Eng. A* **493**, 26 (2008).

<sup>12</sup>Y. Yang, G. P. Li, G. M. Cheng, H. Wang, M. Zhang, F. Xu, and K. Yang, *Scripta Mater.* **58**, 9 (2008).

- <sup>13</sup>R. J. Talling, R. J. Dashwood, M. Jackson, and D. Dye, *Acta Mater.* **57**, 1188 (2009).
- <sup>14</sup>D. C. Chrzan, M. P. Sherburne, Y. Hanlumyuang, T. Li, and J. W. Morris, *Phys. Rev. B* **82**, 184202 (2010).
- <sup>15</sup>T. Furuta, S. Kuramoto, J. Hwang, K. Nishino, and T. Saito, *Mater. Trans.* **46**, 3001 (2005).
- <sup>16</sup>M. Besse, P. Castany, and T. Gloriant, submitted to publication (2011).
- <sup>17</sup>E. Furubayashi, *J. Phys. Soc. Jpn.* **27**, 130 (1969).
- <sup>18</sup>P. Castany, F. Pettinari-Sturmel, J. Crestou, J. Douin, and A. Coujou, *Acta Mater.* **55**, 6284 (2007).
- <sup>19</sup>See EPAPS Document No. [number will be inserted by publisher] for supplementary movie 1 (motion of screw dislocations). For more information on EPAPS, see <http://www.aip.org/pubservs/epaps.html>.
- <sup>20</sup>F. Louchet, L. P. Kubin, and D. Vesely, *Philos. Mag. A* **39**, 433 (1979).
- <sup>21</sup>D. Caillard, *Acta Mater.* **58**, 3504 (2010).
- <sup>22</sup>S. Farenc, D. Caillard, and A. Couret, *Acta Metal. Mater.* **43**, 3669 (1995).
- <sup>23</sup>J. Douin, P. Castany, F. Pettinari-Sturmel, and A. Coujou, *Acta Mater.* **57**, 466 (2009).
- <sup>24</sup>R. J. Talling, R. J. Dashwood, M. Jackson, S. Kuramoto, and D. Dye, *Scripta Mater.* **59**, 669 (2008).
- <sup>25</sup>J. Douin, P. Veyssi re, and P. Beauchamp, *Philos. Mag. A* **54**, 375 (1986).
- <sup>26</sup>J. Douin, <http://www.cemes.fr/Personnel/douin/Disdi-Page.html>.
- <sup>27</sup>See EPAPS Document No. [number will be inserted by publisher] for supplementary movie 2 (motion of non-screw dislocations). For more information on EPAPS, see <http://www.aip.org/pubservs/epaps.html>.
- <sup>28</sup>S. Stoyan, W. S. Kendall, and J. Mecke, *Stochastic Geometry and its Applications* (Wiley, Chichester, New York, 2008).

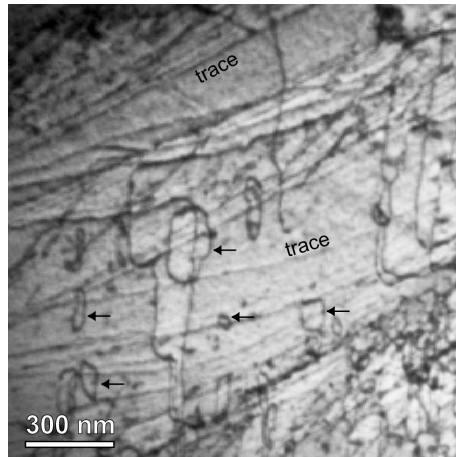


FIG. 1. Mobile dislocations produced during *in situ* tensile test; black arrows indicate expanding dislocation loops created via double cross-slip; some slip traces are also indicated.

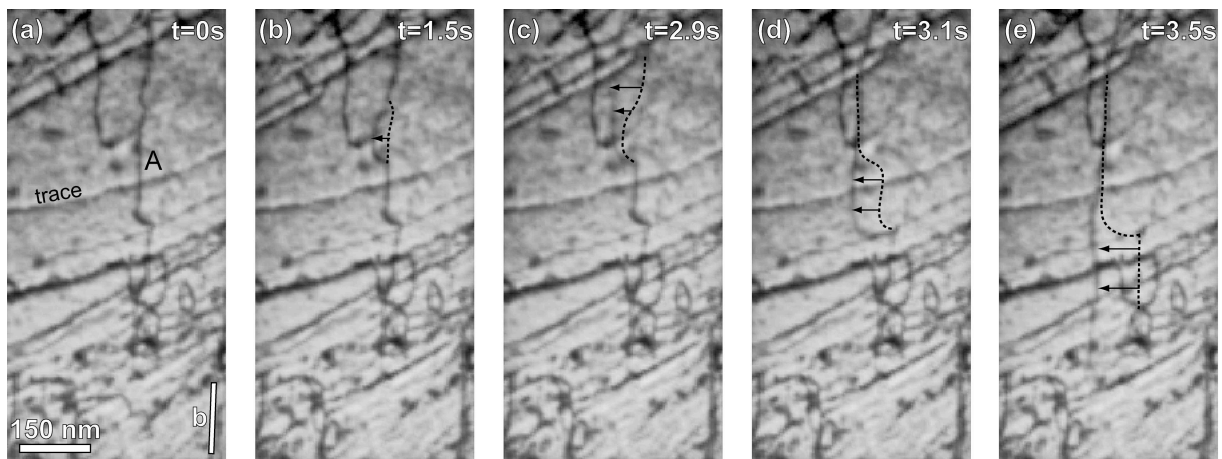


FIG. 2. Typical motion of a screw dislocation (indicated A) during *in situ* TEM tensile test; on each frame, the previous position of the moving part of the dislocation is highlighted with dashed lines; the black arrows indicate the direction of slip; the tensile direction lies along the vertical direction of the figure.

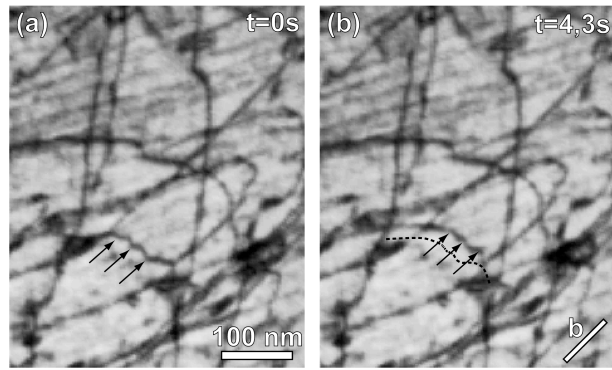


FIG. 3. Motion of non-screw segments showing unresolved pinning points (arrows);  $b$  is the projection of the Burgers vector in the observation plane.